Supporting Information

Computation of a Theoretical Membrane Phase Diagram, and the Role of Phase in Lipid Raft-Mediated Protein Organization

Eshan D. Mitra[†1], Samuel C. Whitehead[‡], David Holowka[†], Barbara Baird[†*], James P. Sethna[‡*]

[†]Department of Chemistry and Chemical Biology, Cornell University, 122 Baker Laboratory, Ithaca, NY, 14853

[‡]Department of Physics, Cornell University, 109 Clark Hall, Ithaca, NY, 14853

*Corresponding authors:

B. Baird, Department of Chemistry and Chemical Biology, Cornell University, 122 Baker Laboratory, Ithaca, NY, 14853; phone: 607-255-4095; email: bab13@cornell.edu

J. P. Sethna, Department of Physics, Cornell University, 109 Clark Hall, Ithaca, NY 14853; phone: 607-255-5132; email: sethna@cornell.edu

[1]Current address: Los Alamos National Laboratory, P.O. Box 1663, Los Alamos, NM 87545

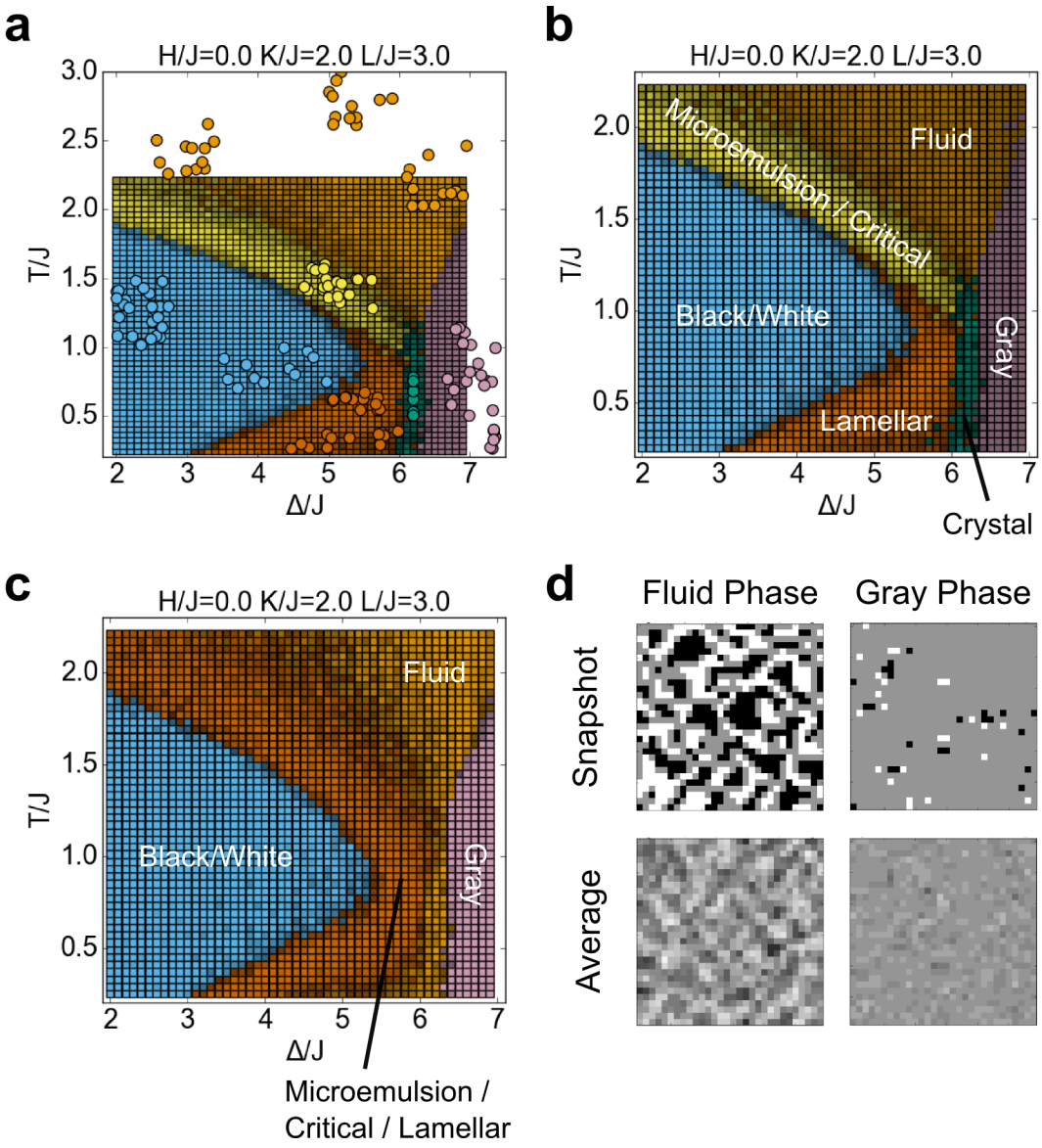

Figure S1: Training the neural network. (a) Each circle at specified (Δ/J, T/J) coordinates represents a parameter set at which training data were acquired. The color indicates the human-generated classification of the phase at that point. These points are overlaid on the final phase diagram computed by the neural network. (b-c) Phase diagrams generated by two types of neural network. (b) is trained on averages of correlated Monte Carlo snapshots to identify all six phases, while (c) is trained on individual Monte Carlo snapshots to identify four phases. Our final phase diagram is based mostly on (b), but we take the classification of the

gray phase from (c) due to its high confidence in that phase. (d) Example simulation images taken near the Fluid / Gray boundary (Fluid at $T/J = 1.49$, $\Delta/J = 6.2$; Gray at $T/J = 1.49$, $\Delta/J = 6.8$), demonstrating the one case in which working with snapshots (phase diagram (c)) is advantageous compared to working with averages (phase diagram (d)). Note that the snapshots shown are easily distinguishable as two different phases, but the averages shown look more similar to each other.

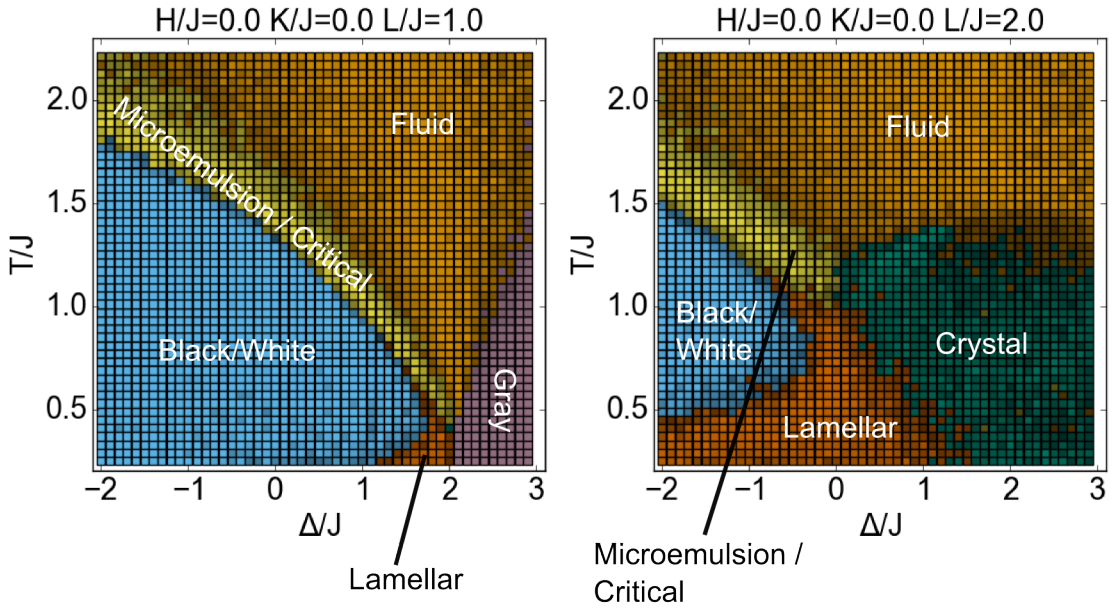

Figure S2: Cross-sections of the phase diagram in which H/J=0, K/J=0, and L/J = 1 or 2. Colors have the same meaning as in Figure 3 and Figure S1.

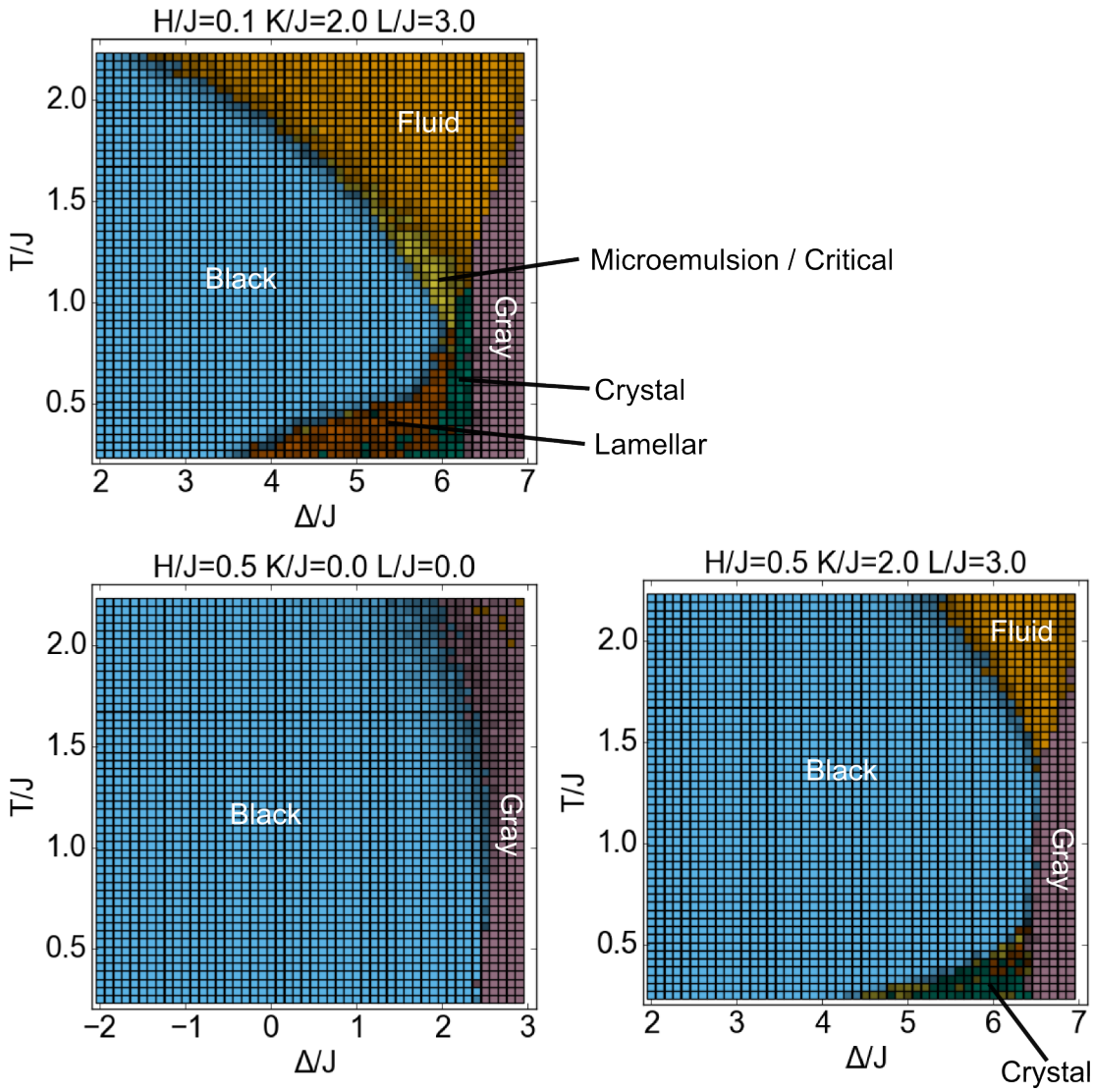

Figure S3: Additional cross-sections of the phase diagram at positive H. Colors have the same meaning as in Figure 3 and Figure S1.

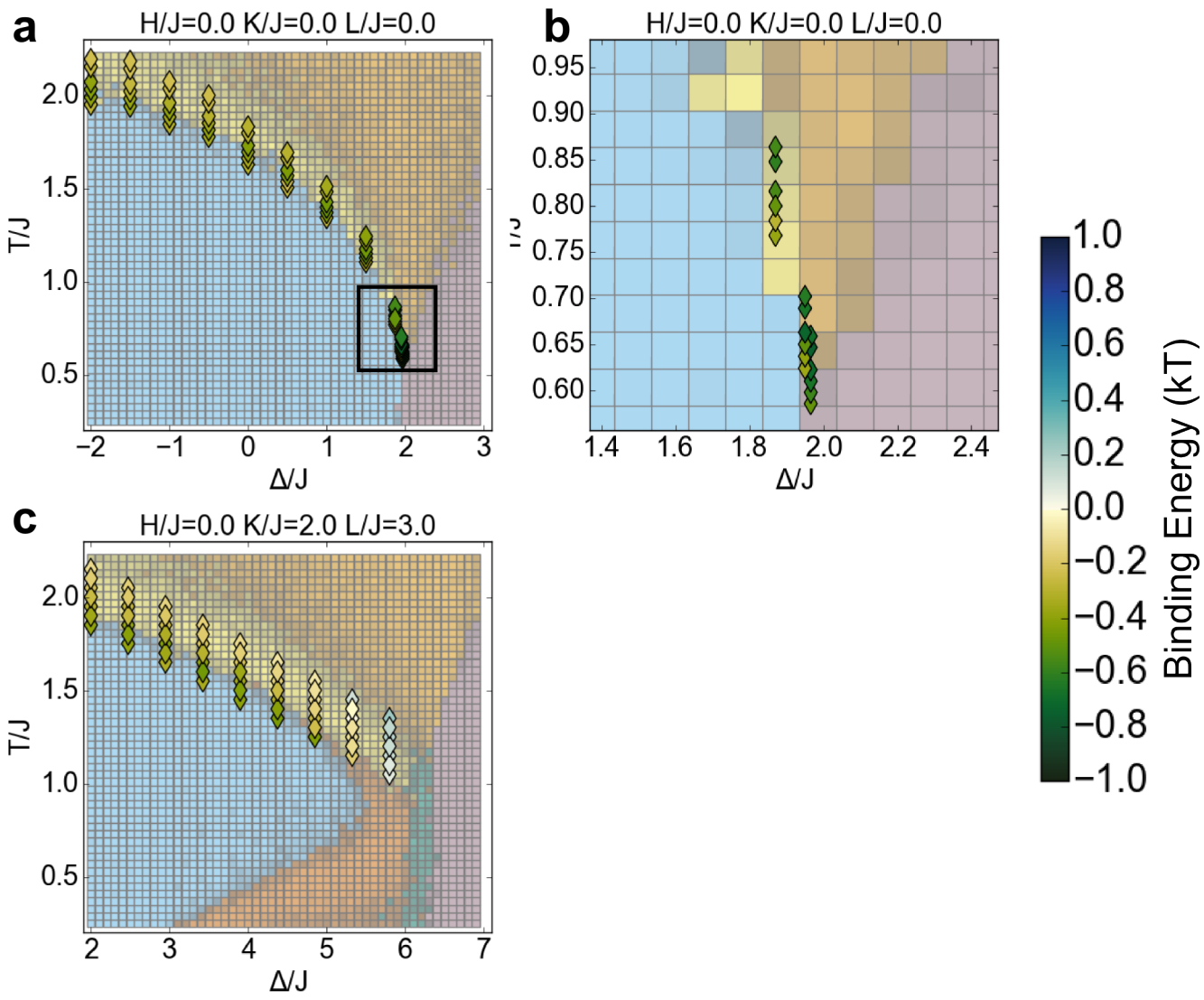

Figure S4: Free energy change (binding energy) due to moving two white pixels to a spacing of 3 lattice units apart. Simulations were run on a system similar to that shown in Figure 5, but with the box on the left containing, instead of the set cluster of 3 IgE receptors (each represented by 12 pixels), a single fixed white pixel. Each diamond indicates the free energy calculated by Bennett's method at that point in the phase diagram. (a) Binding energy in the Blume-Capel model (H=0, K=0, L=0) cross-section. (b) Inset of (a) in the area of the tricritical point (black box in (a)). Similar to the more complicated case of clustered receptors (Figure 6a-b), the binding energy is considerably higher close to the tricritical point. (c) Binding energy

in a cross-section that includes microemulsions ($K/J = 2$, $L/J = 3$). Similar to the more complicated case (Figure 6d), certain microemulsions give a positive binding energy. We provide data for this case, which is simpler than that shown in the main text, in the hopes that it will prove useful for future theoretical work related to this model. In particular, we note that it may be possible develop a universal scaling theory to describe the increase in binding energy magnitude as the tricritical point is approached.

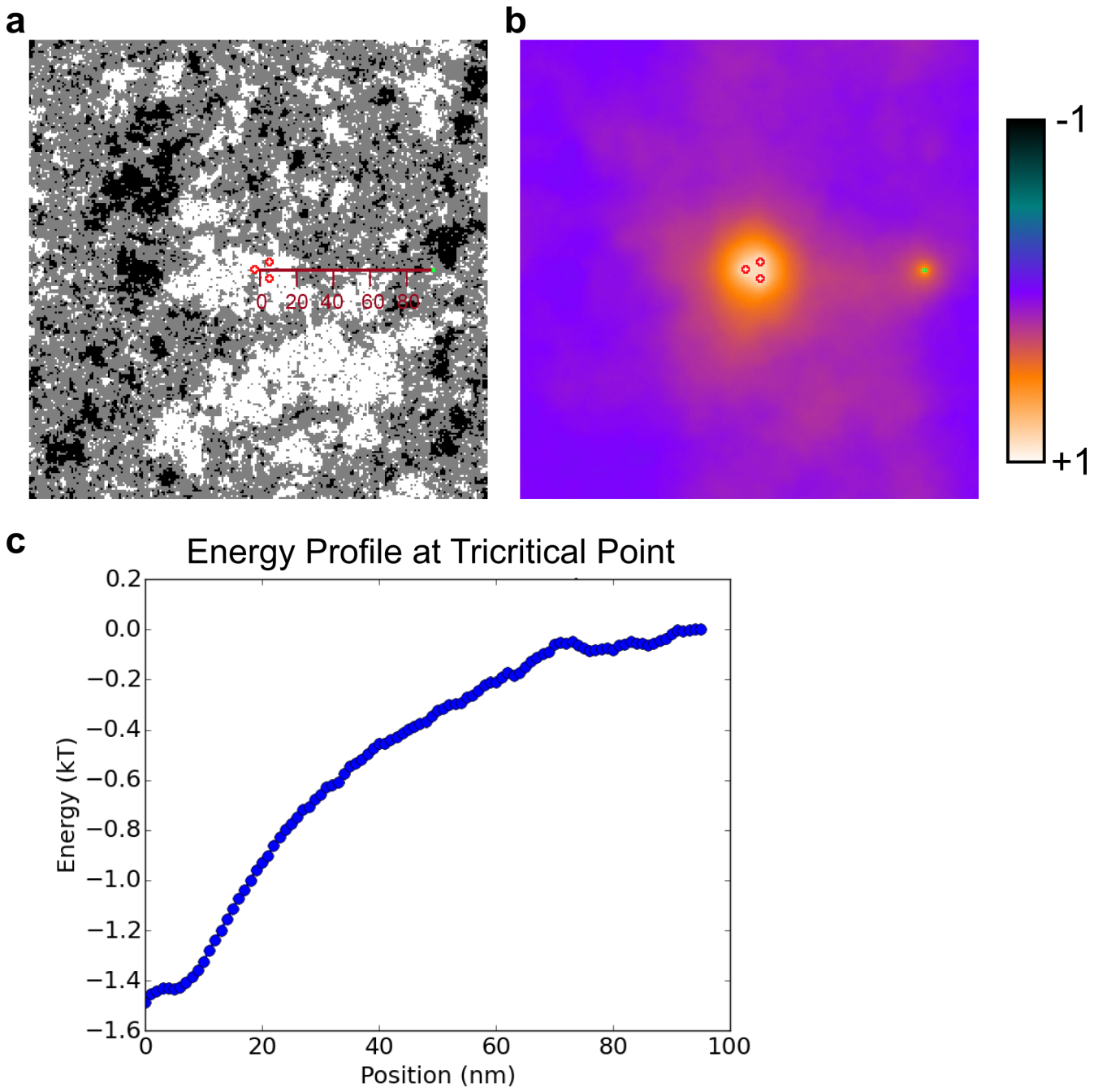

Figure S5: Alternate method for calculating kinase binding energy. We use the method described in [1]. (a-b) Example simulation at the tricritical point, in which the kinase sits at a position 95 nm from the cluster. As in Figure 5, receptors (red) and kinase (green) were held fixed as white, and the rest of the lattice was Monte Carlo sampled. (a) shows one simulation snapshot, and (b) shows the average of all snapshots acquired. The simulation was repeated

at every possible kinase position from 0 to 95, stepwise, in order to generate (c), the profile showing the free energy of the kinase in every position. The position axis in (c) corresponds to the axis shown in (a). The free energy at position 3 nm of ~ -1.4 k_BT is in good agreement with the computationally cheaper method used in the rest of the study (Figure 6, Figure S4).

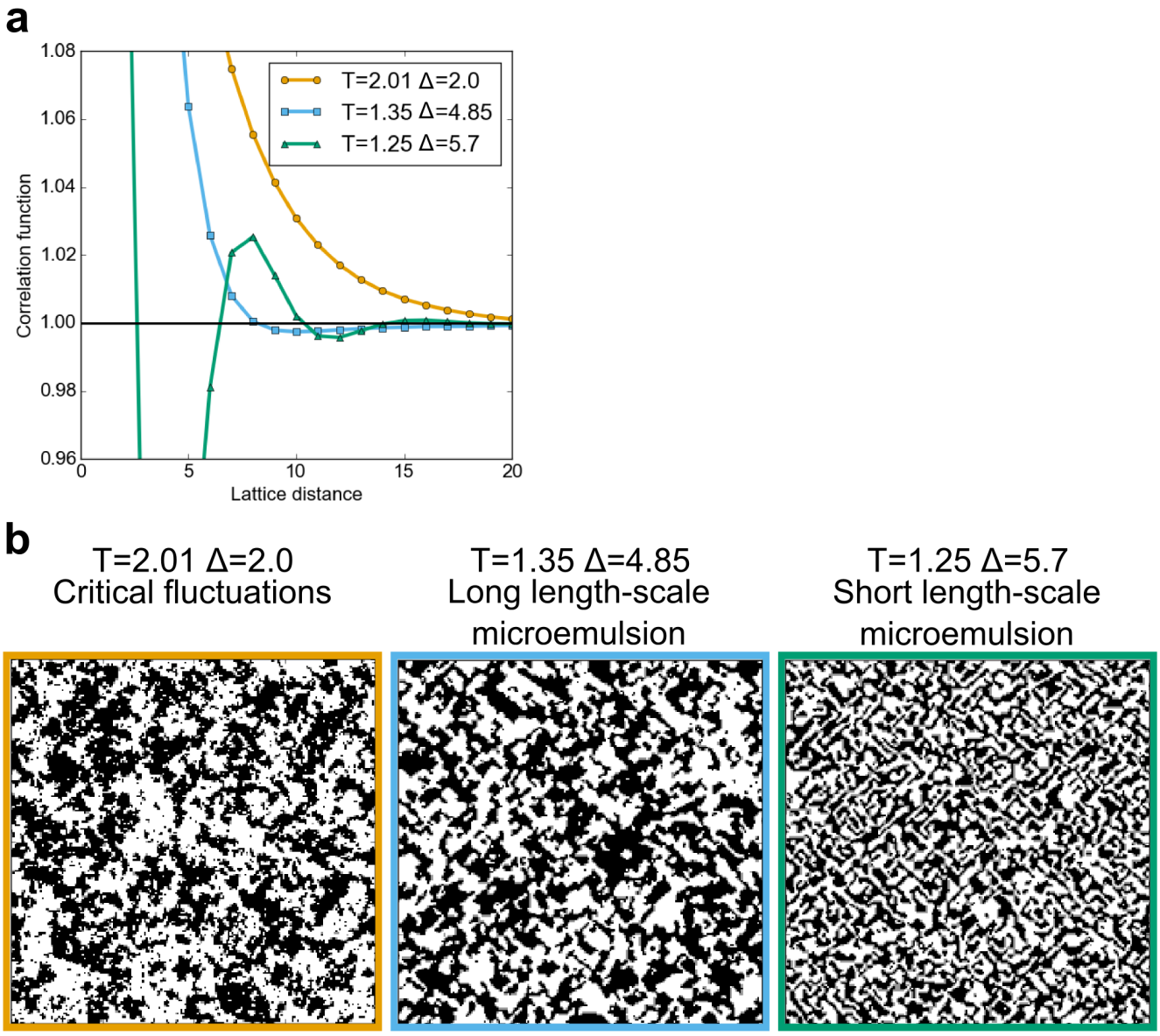

Figure S6: Detailed analysis of three selected points in the *H*/*J*=0, *K*/*J*=2, *L*/*J*=3 cross-section. (a) Correlation functions between white pixels at the selected points. The 2D correlation functions *G* are calculated according to the formula

$$G = \frac{1}{\rho^2} \frac{FFT^{-1}\left(\left|FFT(A)\right|^2\right)}{FFT^{-1}\left(\left|FFT(M)\right|^2\right)}$$

where *A* is a 2D array with value 1 if the *σ* value at the corresponding pixel of the snapshot is 1 (white pixel), or 0 otherwise, *M* is an array of all 1's of the same size as *A*, *ρ* is the density of

white pixels (calculated as the sum of *A* divided by the sum of *M)*, and FFT represents the fast Fourier transform. A correlation function value greater than 1 indicates positive correlation, 1 indicates no correlation, and less than 1 indicates anticorrelation. The function plotted here is the average transect of *G* along the horizontal (1,0) and vertical (0,1) directions (used instead of a radial average because *G* is not always radially symmetric). Correlation functions are averaged over 2000 snapshots of size 200x200 per point.

One criterion to define a microemulsion is that this correlation function must have a local minimum, rather than decrease monotonically. By this criterion, T=2.01, Δ=2.0 is not a microemulsion, as the correlation function decreases monotonically. T=1.35, Δ=4.85 is a microemulsion with length scale ~ 10 because the first local minimum occurs at lattice distance 10, and T=1.25, Δ=5.7 is a microemulsion with length scale ~ 4 because the (considerably stronger) first local minimum occurs at lattice distance 4. (b) The analysis using correlation functions gives results consistent with a visual inspection of snapshots at the same three points, which appear as critical fluctuations (left), a long length-scale microemulsion (center), and a short length-scale microemulsion (right).

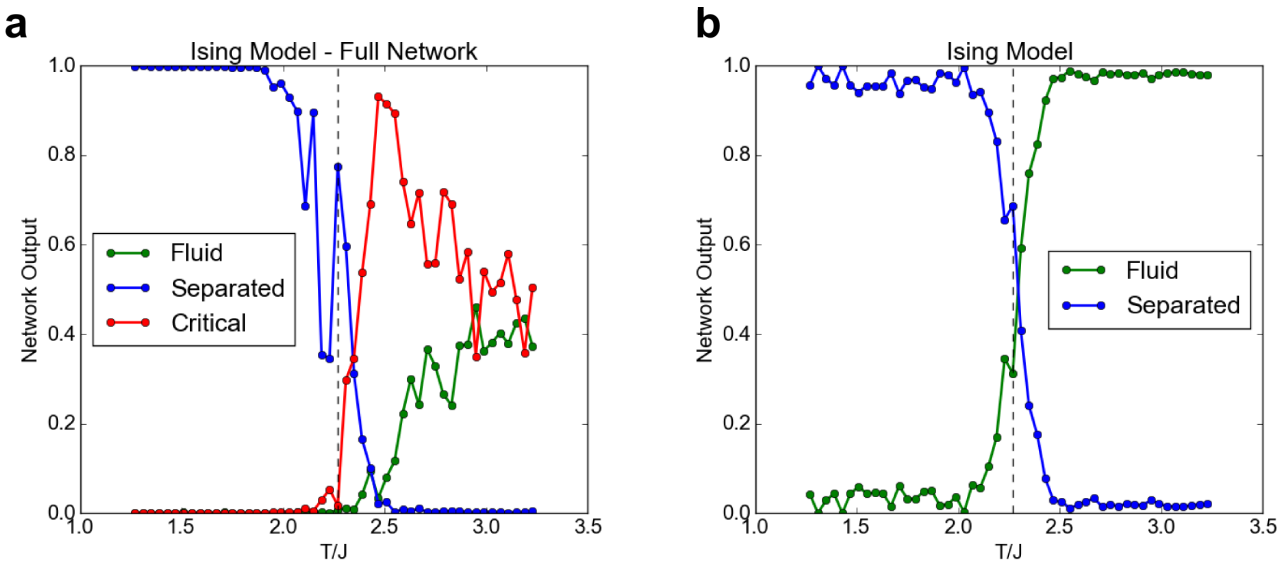

Figure S7: Neural network computation of the Ising model phase diagram. Graphs show the outputs of the neural network corresponding to each phase, indicating the network's level of confidence that the system represents that phase. At each temperature value, the network's prediction is the phase for which the network output is the highest. The true Ising transition temperature is indicated by the dashed line; an accurate network should give “Separated” as the highest output below this temperature, and “Critical” or “Fluid” as the highest output above this temperature. (a) Output of the neural network used in the rest of this study. The predicted transition temperature is close to, but slightly above, the true transition temperature. (b) Output of a neural network specialized for the Ising model only. This network was trained on examples from the Ising model, and only distinguishes between the fluid and phase-separated states. This network's predicted transition temperature almost exactly matches the true transition temperature.

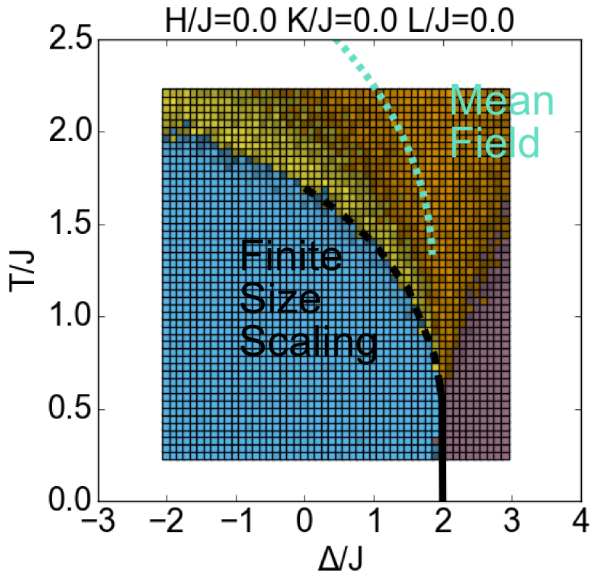

Figure S8: Comparison to other methods for calculation of the Blume-Capel phase diagram. The neural network's phase diagram follows the same key as in Figure 2. Overlaid in gray is the phase boundary as determined by finite size scaling in [2]. The dashed line represents a critical phase transition, solid represents a first-order transition, and the transition from dashed to solid is the tricritical point. Dotted line in blue is the critical line as determined by mean field theory in [3].

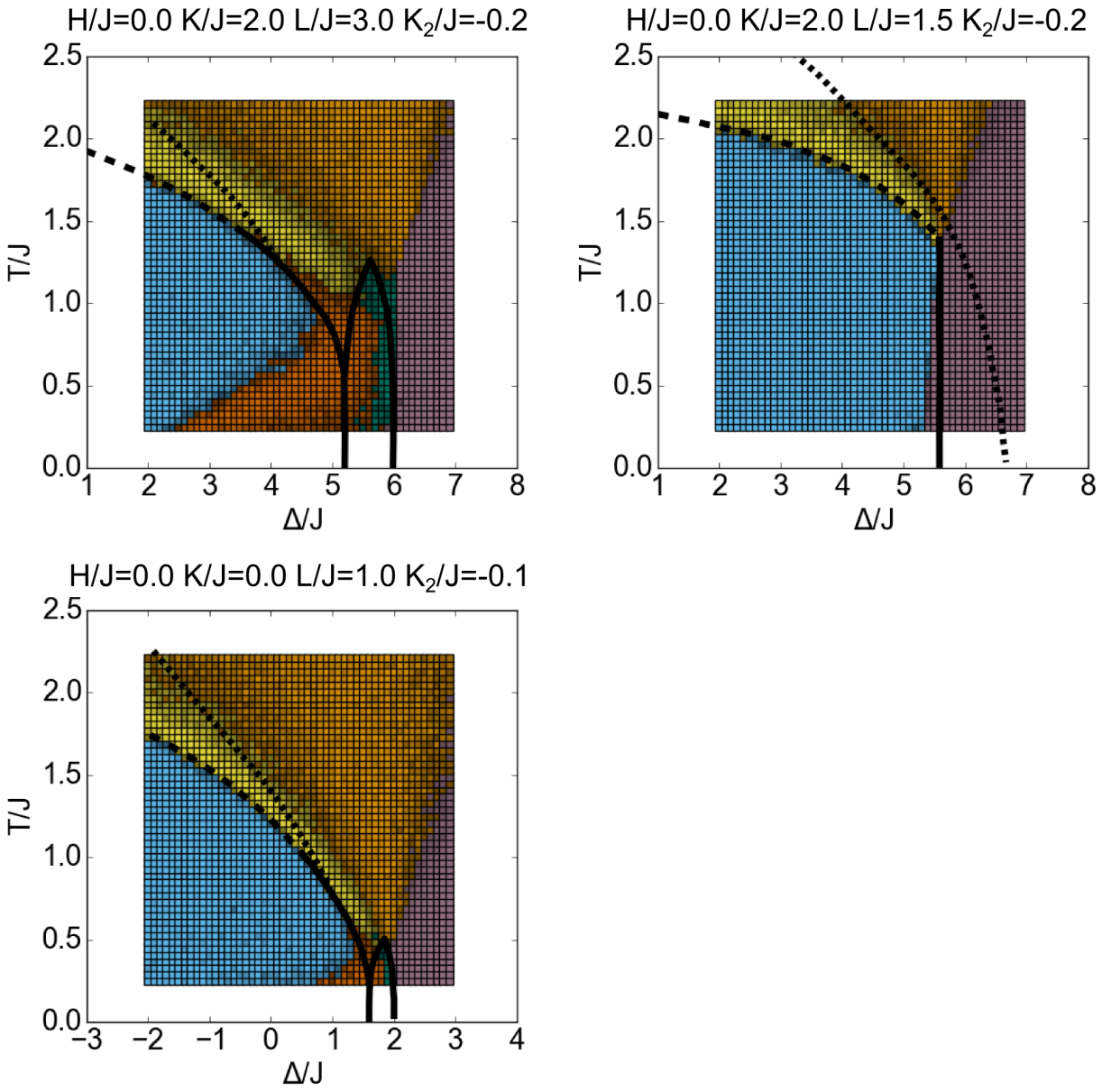

Figure S9: Comparing phase diagram results from our study to the original study. Gray overlays are reproduced from the original study.[4] Solid lines indicate first order phase transitions, dashed lines indicate critical phase transitions, and dotted lines are Lifshitz lines.

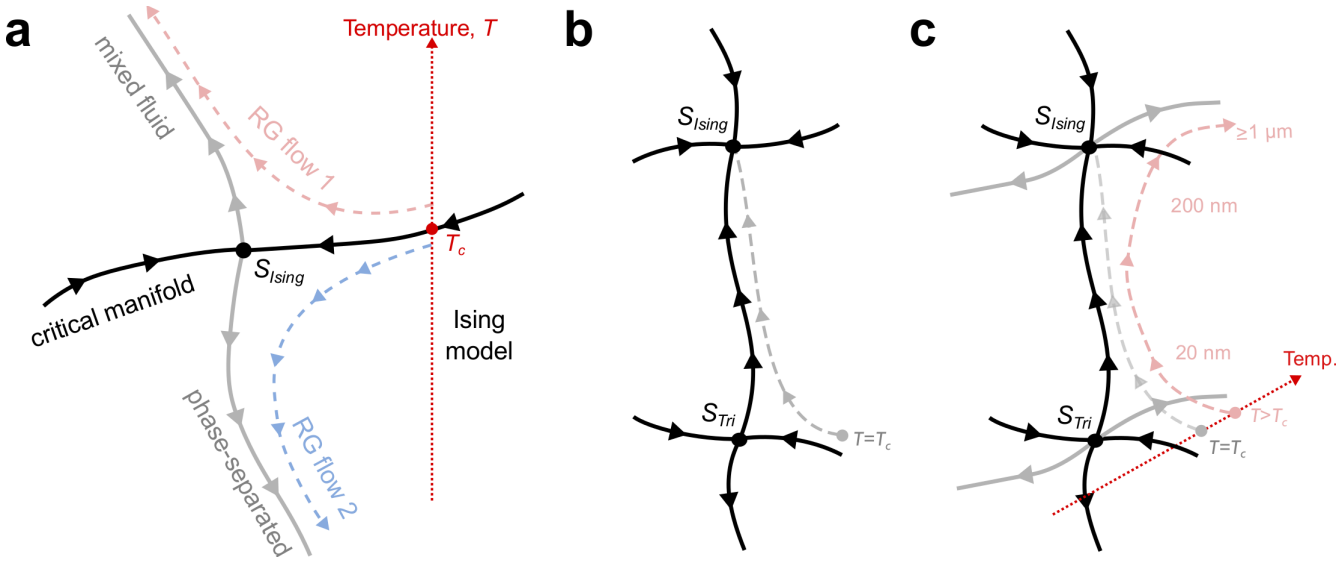

Figure S10: Schematic of renormalization group flows and crossover behavior. The operation of coarse-graining leads to flows through the space of possible models (i.e. a space whose different directions correspond to different model parameters), a process formalized by the renormalization group (RG). Fixed points in this model space are models that look the same at all length scales, and correspond to different classes of critical phenomena. (a) gives an example of RG flows in the familiar Ising model. S_{Ising} is the Ising critical fixed point; under coarse-graining, models flow towards it along black lines and away along gray lines. For the Ising model, temperature (vertical, dotted red arrow) is crucial in determining model behavior. Above the critical temperature, T_c, as we coarse-grain our model (RG Flow 1), it flows to a mixed (uniform) fluid state. Below T_c (RG Flow 2), the model flows toward a phase-separated state. Importantly, when the models in either RG Flow 1 or 2 pass near S_{Ising}, they exhibit Ising-like properties, and coarse-graining to length scales of 20 nm is typically sufficient to produce critical behavior. (b) In the presence of more than one critical fixed point, a model's trajectory through RG flows can pass near—and thus be influenced by—the multiple different fixed points. In this schematic, we imagine the trajectory of a membrane model in such a space (gray dashed arrow), where S_{Tri} and S_{Ising} are the 2D tricritical and 2D Ising critical fixed

points (respectively). At $T=T_c$, where T_c is the Ising critical temperature, the model flows directly to the Ising fixed point. The transition from tricritical-like to Ising-like behavior is referred to as crossover. (c) In the same space as (b), above T_c, our model can flow along a complicated trajectory (red dashed arrow line). Note that here we have included a 3rd dimension—temperature, which acts as in (a). At short length scales (~20 nm), our model is near the tricritical fixed point, and will thus obey tricritical behavior. As we coarse-grain further, our model flows away toward the Ising critical point, so that the behavior of the model at intermediate length scales (~200 nm) is Ising-like. As we coarse-grain even further, the model flows away to some non-critical fixed point.

Supporting References

(1) Machta, B. B.; Veatch, S. L.; Sethna, J. P. Critical Casimir Forces in Cellular Membranes. *Phys. Rev. Lett.* **2012**, *109* (13), 138101.

(2) Beale, P. D. Finite-Size Scaling Study of the Two-Dimensional Blume-Capel Model. *Phys. Rev. B* **1986**, *33* (3), 1717–1720.

(3) Blume, M.; Emery, V. J.; Griffiths, R. B. Ising Model for the λ Transition and Phase Separation in He3-He4 Mixtures. *Phys. Rev. A* **1971**, *4* (3), 1071–1077.

(4) Gompper, G.; Schick, M. Lattice Model of Microemulsions: The Effect of Fluctuations in One and Two Dimensions. *Phys. Rev. A* **1990**, *42* (4), 2137–2149.